

Enhanced lithium storage and chemical diffusion in metal-LiF nanocomposites: Experimental and theoretical results

Yuri F. Zhukovskii,^{1,2} Palani Balaya,^{1,3} Mickael Dolle,¹ Eugene A. Kotomin,^{1,2} and Joachim Maier¹

¹Max-Planck-Institut FKF, Heisenbergstrasse 1, D-70569 Stuttgart, Germany

²Institute for Solid State Physics, University of Latvia, Kengaraga Strasse 8, Riga LV-1063, Latvia

³Engineering Science Programme, National University of Singapore, Singapore 117574, Singapore

(Received 2 February 2007; revised manuscript received 24 July 2007; published 13 December 2007)

An extra storage of Li has been observed experimentally at low potential in Me/LiF nanocomposites (where Me refers to transition metals such as Cu, Co, etc.), with a pseudocapacitive behavior characterized by a high rate performance. To understand the mechanistic details of the lithium storage anomaly, we have performed comparative *ab initio* calculations on the atomic and electronic structure of the nonpolar Cu/LiF(001) and model Li/LiF(001) interfaces. For this aim, we inserted extra Li atoms at several possible sites of the periodic two-dimensional Me/LiF (Me=Cu,Li) interfaces. The energetically most favorable site for extra Li atom is above the surface F⁻ ion with Cu atoms on the other side of the interface, atop the surface Li⁺ ions. An increase of the inserted Li atom concentration in the Cu/LiF interface is accompanied by an increase of the electron charge transfer from extra Li atoms toward the transition metal adlayers, in agreement with a recently proposed mechanism of interfacial charge storage. This is supported by an analysis of the densities of states projected on different atoms including extra Li, as a function of inserted Li concentration. The Cu/LiF(001) interface permits an insertion of only one monolayer of extra Li atoms, unlike Li bilayer in the case of Ti/Li₂O(111). Diffusion of the excess Li along the interface is found to be accelerated, owing to the splitting of the individual pathways for Li⁺ and e⁻, which explains a high rate performance observed experimentally at low potential. We also compare theoretical estimate and experimental capacity results in the Cu/LiF nanocomposite.

DOI: 10.1103/PhysRevB.76.235414

PACS number(s): 82.47.Aa, 82.45.Yz, 71.15.-m, 73.40.Ns

I. INTRODUCTION

Continuously increasing needs in mobile electronic devices require improved Li-ion batteries.¹ One important demand is the increase of the storage capacity of cathode and anode materials. In this context, the conversion reaction introduced recently in transition metal oxides² is considered to be an important step forward. High lithium storage (800–1200 mA h g⁻¹) was observed in nanocomposites with several metal oxides (CoO, NiO, FeO, RuO₂, etc.) using a reversible conversion reaction that involves their reduction to nanosize transition metals with *in situ* formation of nanoscale Li₂O.^{2,3} A similar heterogeneous conversion reaction was also reported in nanocomposites with fluorides, such as TiF₃, FeF₂, BiF₃, etc.^{4,5} Moreover, in both Me/Li₂O and Me/LiF nanocomposites, an additional pseudocapacitive lithium storage (75–150 mA h g⁻¹) was observed at low potentials.

To explain the origin for the latter Li storage anomaly, an *interfacial charge storage mechanism* was suggested recently,⁶ which is of great fundamental significance as (i) it highlights the importance of synergistic considerations in composite systems and (ii) it forms the bridge between *capacitor* and *electrode function*. According to this mechanism, Li⁺ ions are stored in the subsurface or surface of Li₂O or LiF, while the electrons (e⁻) are accommodated in the transition metal, thus resulting in a charge separation. In nanostructured solids, such interfacial effects can play a dominant role due to their substantial proportion of interfaces with respect to the bulk (to several tens of vol %) but even more noticeably because of their finite spacing leading to the size effects.⁷ It is important to note that interfacial storage is ob-

served in the Me/LiX (X=O,F) nanocomposites in which no alloy reaction occurs between the transition metal and Li. To stress it again, as both components (Me and LiX matrix) cannot store Li in their bulk, it is the synergistic *two-phase effect* that enables the extra storage at low potential.⁶

In a recent publication,⁸ we provided evidence for such an interfacial storage anomaly in nanocomposites through first principles electronic structure calculations performed on the Ti(0001)/Li₂O(111) model interface. This was found theoretically to be the most stable one amongst the Me/Li₂O interfaces due to a small lattice mismatch and structural compatibility between components, notwithstanding the fact that Ti/Li₂O nanocomposites were not yet experimentally grown. Present calculations are performed on the Cu/LiF(001) and Li/LiF(001) interfaces, which complement our experimental results.^{4,5} Even though the interfacial storage in LiF is less favorable than in Li₂O according to experiments²⁻⁵ and structural expectations, we concentrate here on the LiF(001) surface, as it is nonpolar in contrast to Li₂O(111) considered in the previous study.⁸ [Note that amongst different densely packed lithium fluoride and lithia substrates both LiF(001) (Ref. 9) and Li₂O(111) (Ref. 10) were found to be energetically most stable, with the lowest surface energy. Thus, they may prevail also in nanocomposites where the ratio surface/volume is much larger than in two-dimensional (2D) slabs.]

In this paper, we shortly present experimental results of lithium storage in the Me/LiX nanocomposite vs Li and compare such low potential extra storage with effects in various nanocomposites such as Ru/Li₂O, Co/Li₂O, and Co/LiF.³⁻⁵ As models of the Me/LiF interfaces, we consider 2D slabs containing a Me (=Cu,Li) overlayer atop the LiF(001) substrate. The number of Cu monolayers is varied

TABLE I. (Color) Atomic charges and energetic parameters of different configurations of 0.25 Li ML inserted into the Cu (bilayer)/LiF(001) (tetralayer) interface. Numbers in brackets are relative energies per extra Li atom for 1 ML coverage of LiF(001) substrate.

Reaction step	Extra Li atom position	Relative energy per extra Li (eV)	The effective charge in different configurations (e)				Graphic images of interfaces
			Extra Li	Li(s)	F(s)	Cu(ad)	
(a) extra Li atom inserted into the Cu/LiF(001) interface	Over F ion	0 (0)	0.90	0.95	-1.0	-0.171	
	Hollow position	0.65 (0.38)	0.88	0.81	-1.0	-0.128	
(b) extra Li atom inserted into the first outermost LiF(001) interlayer	Octahedral position	3.07 (unstable)	0.82	0.80	-1.0	-0.076	
(c) extra Li atom on the LiF(001) plane opposite to Cu/LiF interface	Hollow position	2.16 (2.74)	0.90	0.72	-1.15	-0.027	
	Under F ion	1.52 (1.89)	0.92	0.80	-1.1	-0.026	

^aExtra Li means the effective charge on an extra Li atom, F(s), Li(s), and Cu(ad) effective charges on the interfacial F and Li ions nearest to inserted Li atom as well as on Cu adatoms, respectively.

^b Cu ● Li⁺ ● F⁻ ● extra Li

between 1 and 3, in order to study the influence of the metal thickness and to compare calculations with the behavior of nanosized metals in real experimental situations.

II. THEORETICAL BACKGROUND

Unlike the polar Li₂O(111) substrate with the stoichiometric substrate slab consisting of two oxygen planes surrounded by two lithium planes each,⁸ the slab model of the nonpolar LiF(001) surface includes four layers consisting of

an equal number of alternating fluorine and lithium ions forming a square 2D lattice (Table I). Both components of Me/LiF(001) interfaces (Me=Cu,Li) possess a cubic lattice structure, which is described by both $Fm\bar{3}m$ (Cu and LiF fcc structures) and $Im\bar{3}m$ space groups (Li bcc structure); i.e., they are symmetrically compatible. However, the lattice constant of the LiF substrate (4.03 Å) noticeably exceeds that for Cu (3.62 Å) and Li (3.51 Å),¹¹ by 10% and 13%, respectively. The thickness of the copper trilayer in our models

(i.e., ~ 0.6 nm) is quite comparable with the size of Ru or Co nanograins observed experimentally.^{2,3} In order to vary the lithium atom concentration at the Cu/LiF(001) interface beginning with the 0.25 ML (monolayer), we have considered 2×2 surface supercells (Table I). Extra Li atoms have been inserted in several positions of the Cu/LiF(001) interface: (i) above the outermost F⁻ ion [Table I(a)], (ii) above the outermost *hollow* position of the Li-F square (the middle of the nearest F-F distance), (iii) inside the outermost LiF interlayer under the hollow position [Table I(b)]. We also calculated Li atoms on the opposite side of the LiF(001) slab [Table I(c)] and simulated analogously the Li/LiF(001) interface.

The structure relaxation of free and Li containing interfaces has been performed using the optimization procedure of the CRYSTAL-03 code.¹² To optimize geometry, we have relaxed the first atomic coordination sphere around the inserted Li atom as well as metal-substrate spacing (Table I). Before Li atoms are inserted into the Cu/LiF interface, the innermost Cu adatoms prefer to sit atop the outermost surface F⁻ ions of a LiF substrate. The same is true when Li atoms are inserted into the Cu/LiF interface in the hollow positions above LiF [Table I(a)]. However, if extra Li atoms (in concentration ≥ 0.25 ML) are inserted atop the surface F⁻ ions, the Cu overlayer is shifted as a whole along the interface, so that the interfacial Cu adatoms sit atop the substrate Li⁺ ions of LiF [Table I(a)]. At the same time, the arrangement of the Li adsorbate is not changed at a small concentration of interfacial extra Li atoms atop F⁻ ions since the density of atoms in the bcc Li monolayer is twice as small as that in the fcc Cu layer.

In our *ab initio* calculations performed with the localized basis set of Gaussian-type orbitals, we have used the hybrid B3PW method, which includes a partial incorporation of the exact Hartree-Fock exchange into the density functional theory (DFT) exchange functional as implemented in the CRYSTAL-03 code.¹² The all-electron basis sets for atomic functions of F ($7s-311sp$) and Li ($3s-1sp$) were earlier optimized for a LiF single crystal,^{13,14} whereas Cu atomic functions (HAYWSC-4111 $sp-31d$) were optimized by us¹⁵ using a small core Hay-Wadt pseudopotential.¹⁶

We prefer the hybrid B3PW method for Me/LiX slab calculations since it gives an accurate band gap for insulators such as LiF.¹² Notice that in recent theoretical studies of electrode materials in Li batteries, such as the study of the electronic and electrochemical properties of $\text{Li}_x(\text{Ni}_{0.5}\text{Mn}_{0.5})\text{O}_2$,¹⁷ the prediction of lithium ordering in Li_xCoO_2 , or the phase separation in Li_xFePO_4 nanocomposites,^{18,19} the alternative DFT plane wave formalism was used as implemented in the VASP code,²⁰ which usually considerably underestimates the band gap. The mechanism of Li insertion reaction in Cu_6Sn_5 (Ref. 21) as well as InSb and Cu_2Sb (Ref. 22) anode materials was successfully investigated recently using the linearized augmented plane wave WIEN-2K code. Such studies have proven the power of the first principles calculations in understanding lithium insertion/intercalation reactions. The present study focuses on understanding the lithium storage at the *interfaces* of Me/Li₂O or Me/LiF nanocomposites using *ab initio* hybrid calculations where experimental techniques have limitations in providing a direct evidence.

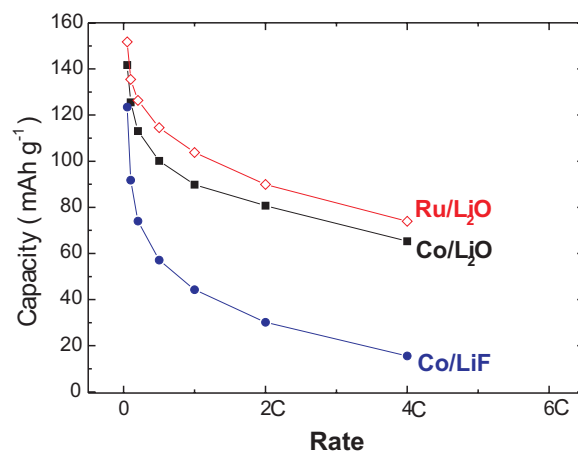


FIG. 1. (Color) Comparison of low potential extra storage in different metal-Li₂O and metal-LiF nanocomposites. It is worthy to note that the storage at very low rates in Co/Li₂O and Co/LiF nanocomposites is predominated by the 10% carbon used along with active electrode as conductive additive, unlike in Ru/Li₂O which has no conductive carbon additive. A 1C rate corresponds to the current rate of 805 mA g⁻¹, which in ideal situation leads to a storage of 4 Li⁺ in 1 h.

III. EXPERIMENTAL STUDY OF EXTRA LI STORAGE AT Me/LiF INTERFACES

Previous experimental studies of a few transition metal fluorides as electrode material evidenced the possibility of a partly reversible high Li storage through a conversion reaction forming Me/LiF nanocomposites.^{4,5} In the case of CuF₂, upon incorporation of 3.1 Li⁺ during the first discharging, a Cu/LiF nanocomposite is formed at a Li storage of 840 mA h g⁻¹. Raman as well as x-ray photoemission spectroscopy (XPS) spectra taken on fully discharged as well as fully charged CuF₂ samples confirmed the presence of Cu/LiF composites upon discharging to 0.02 V and of nanocrystalline CuF₂ phase upon charging to 4.3 V. However, a complete conversion of the Cu/LiF nanocomposite to CuF₂ was found to be difficult to achieve; only 1 Li⁺ could be removed upon the first charging corresponding to about 38% of Coulomb efficiency.⁴ If the charge-discharge of the Cu/LiF nanocomposite is limited to the voltage window of 0.02–1.0 V, a pseudocapacitive behavior with a reasonably good cyclic performance is achieved. When cycling at a rate of C/20 in this low potential window, Li storage of about 113 mA h g⁻¹ is observed (after correction with respect to 10% of carbon content in the electrode). Within this voltage window, no change in the valence state of Cu is observed from the XPS measurements upon discharging and charging, referring to the lithium storage in this voltage window not related to the redox reaction associated with the insertion or conversion reaction but solely due to an interfacial adsorption and desorption phenomenon.

As discussed earlier,⁸ such a low potential extra storage can be achieved even at a faster rate of discharge and charge cycling. Figure 1 presents a comparison of rate performances of extra lithium storage within a voltage window of 0.02–1.2 V for selected metal-Li₂O and metal-LiF nanocomposites. Among them, Ru/Li₂O (without any carbon ad-

TABLE II. Dependence of the charge transfer across the Cu/LiF(001) interface on a number of Cu fcc adlayers for inserted (extra) Li monolayer over the outermost F^- ions (see footnote in Table I).

Cu monolayer for 1 extra Li ML				Cu bilayer without extra Li			Cu bilayer for 1 extra Li ML				Cu trilayer for 1 extra Li ML			
Extra Li	F(s)	Li(s)	Cu(ad)	F(s)	Li(s)	Cu(ad)	Extra Li	F(s)	Li(s)	Cu(ad)	Extra Li	F(s)	Li(s)	Cu(ad)
0.94	-1.0	0.71	-0.63	-0.98	0.97	0.02	0.93	-1.0	0.74	-0.67	0.91	-1.0	0.78	-0.69

ditive) exhibits high interfacial lithium storage of 152 and 74 mA h g^{-1} at a rate of $C/20$ and $4C$, respectively. The comparison of the interfacial storage in Co/Li₂O and Co/LiF nanocomposites in Fig. 1 suggests a reduced storage capacity if Li₂O is replaced by LiF.

IV. THEORETICAL STUDY OF EXTRA Li IN Me/LiF(001) INTERFACES

The energetically most favorable position for the interfacial Li insertion is found to be above the F^- ions on the Cu/LiF interface, whereas the hollow sites are less favorable for extra Li location [Table I(a)]. The difference between the corresponding energies is 0.65 and 0.38 eV for 0.25 and 1 ML concentration of extra Li, respectively—decrease of the latter is due to a 1 Li ML screening of the Cu-F attraction across the interface. For 0.25 extra Li ML atop the outermost F^- ions, the structural optimization of the copper overlayer (Table I) shows negligible downward displacements of the interfacial Cu atoms toward the surface Li atoms of the LiF substrate, whereas the binding energies of interfacial extra Li (0.25 ML) exceeds those for a 1 ML coverage only by 0.15 eV (per atom).

The energy gain due to insertion of Li atoms into the hollow positions at the Cu/LiF(001) interface [the Cu|Li|LiF structure for the Cu bilayer and 0.25 extra Li ML, as shown in a lower window of Table I(a)] is 4.9 eV. This is energetically more favorable than bringing extra Li at the same concentration into similar positions either atop the copper bilayer (Li|Cu|LiF structure, the adsorption energy of 3.5 eV) or below the LiF(001) slab [Cu|LiF|Li with the adsorption energy of 3.3 eV, the upper window in Table I(c)]. This is a result of Cu stabilization of Li adsorption on the LiF surface. At larger concentrations of extra Li (0.5 ML), the interfacial energy gain is reduced down to 4.2 eV. As soon as the extra Li concentration reaches 1 ML inside the interface between lithium fluoride and transition metal (i.e., all F^- ions are saturated by inserted Li atoms), attempts of further insertion of Li atoms turn out to be energetically unfavorable. That is, on a pure energetic basis, more than 1 Li ML *cannot* be inserted into the Cu/LiF(001) interface.

For the Li/LiF(001) interface, the estimated interfacial energy gains are much smaller: 2.8 and 2.4 eV for 0.25 and 0.5 extra Li ML, respectively, which indicates a rather destabilizing influence of bcc Li monolayer on the insertion of additional Li atom [unlike the Cu/LiF(001) interface and previously studied Li adsorption on the Li₂O(111) surface⁸], whereas the presence of two and three bcc Li layers atop the LiF surface reveals abnormal charge redistribution from the

outermost layer of the Li slab toward the interface. Beyond one extra Li monolayer inside the Li/LiF interface, it is found to be energetically unstable.

Based on the cohesive energy of 2.0 eV for bulk Li [which we calculated using the same computational procedures as well as Li parameters as described in Sec. II; compare the experimental value of 1.7 eV (Ref. 23) and 1.6–2.0 eV obtained in various DFT calculations²⁴], the voltage for the Cu/LiF composites could be estimated in the limit of low Li concentrations as 2.9 and 2.2 V (vs solid Li) for Li interfacial concentrations of 0.25 and 0.5 ML, respectively. One can see a considerable decrease in voltage with the Li concentration increase. For the Li/LiF interface, the estimated voltage is much smaller: 0.8 and 0.4 V for the same extra Li concentration. As soon as Li concentration approaches 1 ML, the voltage here also approaches zero and even becomes slightly negative; that is, the transfer of the Li atom from lithium bulk to the Li/LiF interface turns out to be energetically unfavorable. While the absolute voltage values may not be directly transferable to the experimental conditions, the discussed trends should.

The analysis of charge redistributions in the Cu/LiF(001) interface (Table I) shows that inserted Li atoms donate a considerable portion of the electron density toward the nearest Li ions (thus reducing their effective charges) and to Cu atoms on the other side of the interface. In the extreme case of Li atoms adsorbed on a pure LiF surface on the opposite side of the Cu interface [Table I(c)], the effective charges of F^- ions slightly exceed $-1e$, which is a known artifact of the Mulliken population analysis.

For a given thickness of the Cu layer, e.g., a bilayer, the electronic charge transfer toward Cu grows steadily with an increase of the interfacial Li concentration: from $0.2e$ (for 0.25 Li ML) through $0.47e$ (for 0.5 Li ML) to $0.67e$ (for 1 Li ML). Without inserted Li, there is practically no electron charge transfer across the Cu/LiF(001) interface (Table II) with Li and F charges close to $\pm 1e$. This is in line with a weak physisorption observed by us earlier for a similar non-polar Cu/MgO(001) interface.²⁵ After the insertion of a small amount of extra Li (up to 0.25 ML), each Li atom donates about $0.9e$ toward both the Cu overlayer and surface Li ions [Table I(a)]. The larger the extra Li concentration, the larger the electronic charge transferred. The insertion of Li atoms into the *octahedral* positions even in the first LiF interlayer is energetically very unfavorable [Table I(b)], whereas Li adsorption on a free LiF surface on the opposite side of the interface is less favorable than its insertion inside the Cu/LiF interface [Table I(c)]. For the Cu/LiF(001) interface containing extra Li concentration up to 1 ML, we

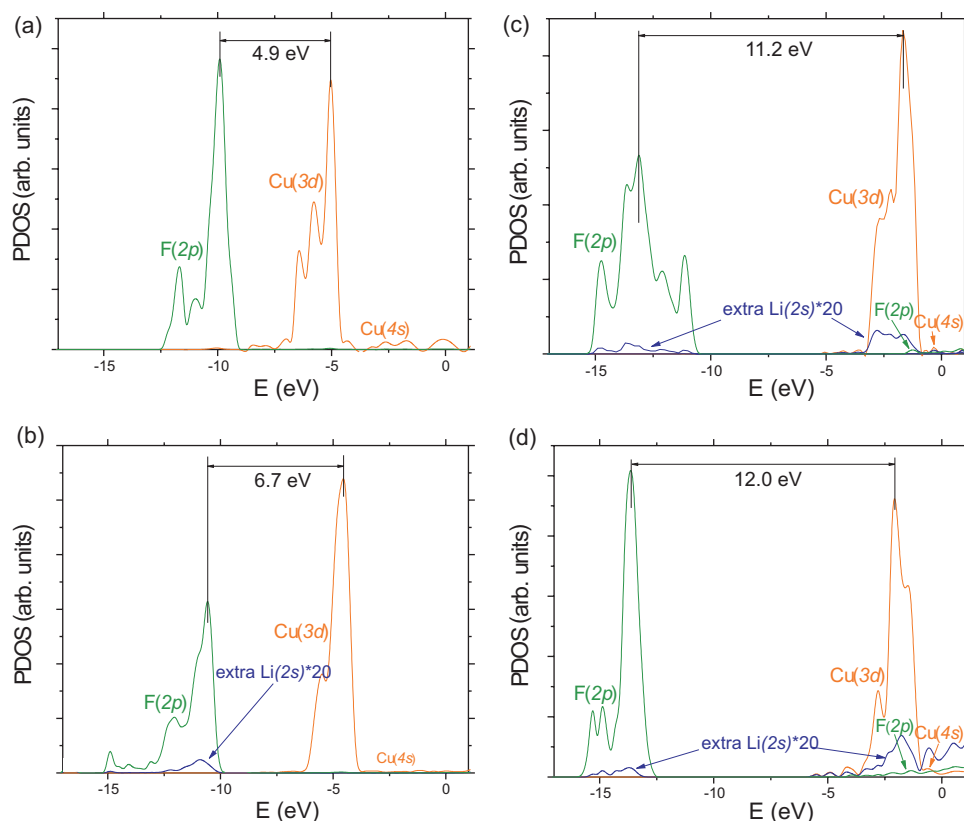


FIG. 2. (Color) DOS projected on F(2p), extra Li(2s), Cu(3d), and Cu(4s) energy states for the four different concentrations of extra Li inside the Cu/LiF(001) interface: 0 ML (a), 0.25 ML (b), 0.5 ML (c), and 1 ML (d). The largest peaks were normalized to the same value, whereas a convolution of individual energy levels was plotted using the Gaussians with a half-width of 0.5 eV.

have observed energetic stability even for a Cu trilayer when the charge transfer achieves up to $0.69e$ per Cu atom for 1 Li ML (Table II). Further growth of the charge transfer (beyond 1 Li ML) toward Cu is hardly possible due to the interface instability for an excess Li content exceeding 1 ML.

The qualitative change of the density of one-electron energy states [density of state (DOS)] as a function of inserted Li concentration in the Cu(bilayer)/Li F(001) interface is shown in Fig. 2 for the energetically favorable position of extra Li atoms atop the surface F^- ions with interfacial Cu adatoms atop the outermost substrate Li ions [Table I(a)]. (As mentioned above, if no Li atoms are inserted, Cu adatoms prefer to sit atop the surface F^- ions.) It is well seen that the positions of the fluorine 2p and copper 3d peaks are very sensitive to the extra Li concentration [see Figs. 2(a)–2(d)]. With an increase of the extra Li concentration (0, 0.25, 0.5, and 1 ML), one observes a substantial growth of the energy difference between the F(2p) and Cu(3d) peaks (pseudogap) for substrate and adsorbate, respectively. This gap achieves 12.0 eV for 1 extra Li ML [Fig. 2(d)], which occurs partly due to the Cu(3d) peak shift to higher energies as a result of increasing electron transfer toward transition metal accompanying the increase of extra Li concentration. This also indicates a weakening of the Cu bonding with the substrate due to the screening effect of the inserted Li layer. Not only a noticeable shift of F(2p), Cu(3d), and Cu(4s) levels along the energy scale is observed with the change of extra Li concentration; the shape of these bands also changes.

As to the projections of Li(2p) states, they are much weaker as compared to both F(2p) and Cu(3d) [analogously

to Mg(3p) states for the Cu/MgO(001) interfaces²⁵]. [The magnified projected DOS intensities for extra Li atoms ($20\times$) are shown in Fig. 2.] The larger the extra Li concentration, the larger the contribution of the extra Li(2p) states just below the Fermi level [zero energy in Figs. 2(a)–2(d)]. These results confirm the Mulliken electron charge donation from the extra Li both toward mainly the interfacial Cu adlayer and partly to the surface Li ions as discussed above and presented in Table II. The Li(2s) states within the area of the F(2p) band arise due to the Pauli expulsion of F states from internal Li area. This is a well known effect caused by the penetration of anion atomic orbitals into the core region of neighboring cations.²⁶

It is also worthy of mention for a comparison that for a bilayer transition-metal coverage of Li_2O substrate⁸ the electronic charge transfer toward Ti was $0.75e$, whereas for the Cu/LiF(001) interface this transfer was found to be slightly smaller, $0.67e$. Since these interfaces have different atomic structures, we cannot compare these results directly. A further increase of the extra Li concentration is quite possible within the Me/Li₂O(111) interface (at least up to bilayer) but is not possible in Me/LiF(001). Indeed, in the case of Li₂O(111), each extra Li atom is located over the hollow position concerning the underneath Li⁺ sublayers, and a total charge on Li⁺ ions is redistributed between Li⁺ ions and inserted neutral Li atoms, in order to reduce interfacial lithium ionicity. On the other hand, the electron charge saturation of the LiF(001) surface by Li⁺ ions positioned over the outermost F^- ions aggravates a further insertion of extra Li atoms (beyond 1 ML) inside the interface. This is in agreement with the difference in lithium storage in the Me/Li₂O(111)

and Me/LiF(001) interfaces observed experimentally (Fig. 1) and explains the difference in Li atom affinity toward Li₂O(111) (Ref. 8) and LiF(001) substrates.

Finally, it is rewarding to briefly consider the Li incorporation kinetics. The activation energies for the *extra Li atom diffusion* along the interface are 0.65 eV for the Cu/LiF(001) and 1.36 eV for the Li/LiF(001). These values as well as 0.81 eV calculated for the Ti/Li₂O(111) interface⁸ indicate that migration energies are quite low. These results shed light on the fact that interfacial storage occurs at a fast rate, as shown in Fig. 2. The fast interfacial storage kinetics is not just due to the low thresholds of Li⁺ transport in LiF, it is also based on the fact that electrons can move fast within the metal during chemical Li transport while they have to accompany the Li⁺ motion in the LiF bulk in the case of intercalation mode. Hence, the heterogeneous storage that allows Li⁺ and e⁻ to sit in preferred phases is also connected with facilitated heterogeneous storage kinetics as both Li⁺ and e⁻ can take their preferred kinetic paths.

V. CONCLUSIONS

We have shown that the extra Li storage capacity obtained in transition metal-LiX (X=O,F) nanocomposites could be explained by an interfacial storage mechanism. Among the Me/LiX (X=O, F; Me=Cu, Ti, Ru, Co) investigated experi-

mentally, the Ru/Li₂O composite exhibits high interfacial storage. Moreover, the Li storage for Co/Li₂O is larger than for the Co/LiF interface. Our theoretical simulations clearly show that this is in line with the different compositions of interfacial Li atoms in the Me/Li₂O and Me/LiF interfaces, corresponding to the different crystal structures. Our DOS analysis semiquantitatively confirms the results of the electronic charge transfer from the LiF substrate toward interfacial copper: the larger the inserted Li concentration, the greater the charge donation, achieving $\sim 0.7e$ per interfacial Cu atom for 1 extra Li ML.

The calculated energy gain for Li atom insertion inside the Cu/LiF(001) interface and, thus, the voltage strongly depend on the inserted Li concentration; both quantities decrease as the Li concentration grows.

The calculated Li migration energy on the Me/LiF interfaces is typically quite small, of the order of 0.5 eV. Evidently, the heterogeneity does not only provide a thermodynamically preferred storage, it is also helpful for the mass transport, as Li⁺ can move along the crystal sites, while the electron takes the metal path.

ACKNOWLEDGMENTS

Authors are indebted to E. Heifets, J. Jamnik, and J. M. Tarascon for fruitful discussions and to the European Union for its support through the ALISTORE project.

-
- ¹I. Buchmann, *Batteries in a Portable World: A Handbook on Rechargeable Batteries for Non-Engineers* (Cadex Electronics, Richmond, BC, Canada, 2001).
- ²P. Poizot, S. Laruelle, S. Grugeon, L. Dupont, and J.-M. Tarascon, *Nature (London)* **407**, 496 (2000).
- ³P. Balaya, H. Li, L. Kienle, and J. Maier, *Adv. Funct. Mater.* **13**, 621 (2003); P. Balaya, A. J. Bhattacharyya, J. Jamnik, Yu. F. Zhukovskii, E. A. Kotomin, and J. Maier, *J. Power Sources* **159**, 171 (2006).
- ⁴H. Li, P. Balaya, and J. Maier, *J. Electrochem. Soc.* **151**, A1878 (2004).
- ⁵H. Li, G. Richter, and J. Maier, *Adv. Mater. (Weinheim, Ger.)* **15**, 736 (2003); F. Badway, F. Cosandey, N. Pereira, and G. G. Amatucci, *J. Electrochem. Soc.* **150**, A1318 (2003).
- ⁶J. Jamnik and J. Maier, *Phys. Chem. Chem. Phys.* **5**, 5215 (2003); J. Maier, *Faraday Discuss.* **134**, 51 (2007).
- ⁷J. Maier, *Nat. Mater.* **4**, 805 (2005).
- ⁸Y. F. Zhukovskii, P. Balaya, E. A. Kotomin, and J. Maier, *Phys. Rev. Lett.* **96**, 058302 (2006).
- ⁹P. W. Tasker, *Philos. Mag. A* **39**, 119 (1979).
- ¹⁰W. C. Mackrodt and P. W. Tasker, *Chem. Br.* **21**, 366 (1983).
- ¹¹R. W. G. Wyckoff, *Crystal Structures*, 2nd ed. (Wiley, New York, 1963), Vol. 1.
- ¹²V. R. Saunders, R. Dovesi, C. Roetti, R. Orlando, C. M. Zicovich-Wilson, N. M. Harrison, K. Doll, B. Civalleri, I. J. Bush, Ph. D'Arco, and M. Llunell, *CRYSTAL-2003 User's Manual*, University of Turin, 2003.
- ¹³R. Nada, C. R. A. Catlow, C. Pisani, and R. Orlando, *Modell. Simul. Mater. Sci. Eng.* **1**, 165 (1993).
- ¹⁴M. Prencipe, A. Zupan, R. Dovesi, E. Aprà, and V. R. Saunders, *Phys. Rev. B* **51**, 3391 (1995).
- ¹⁵Yu. F. Zhukovskii, E. A. Kotomin, and G. Borstel, *Vacuum* **74**, 235 (2004).
- ¹⁶P. J. Hay and W. R. Wadt, *J. Chem. Phys.* **82**, 299 (1985).
- ¹⁷A. Van der Ven and G. Ceder, *Phys. Rev. B* **59**, 742 (1999).
- ¹⁸A. Van der Ven and G. Ceder, *Electrochem. Commun.* **6**, 1045 (2004).
- ¹⁹F. Zhou, C. A. Marianetti, M. Cococcioni, D. Morgan, and G. Ceder, *Phys. Rev. B* **69**, 201101(R) (2004).
- ²⁰G. Kresse and J. Furthmüller, *VASP the Guide*, University of Vienna, 2003.
- ²¹S. Sharma, L. Fransson, E. Sjöstedt, L. Nordström, B. Johansson, and K. Edström, *J. Electrochem. Soc.* **150**, A330 (2003).
- ²²S. Sharma, J. K. Dewhurst, and C. Ambrosch-Draxl, *Phys. Rev. B* **70**, 104110 (2004).
- ²³K. A. Gschneider, Jr., *Solid State Phys.* **16**, 276 (1964).
- ²⁴K. Doll, N. M. Harrison, and V. R. Saunders, *J. Phys.: Condens. Matter* **11**, 5007 (1999).
- ²⁵Yu. F. Zhukovskii, E. A. Kotomin, D. Fuks, S. Dorfman, A. M. Stoneham, and G. Borstel, *J. Phys.: Condens. Matter* **16**, 4881 (2004).
- ²⁶J. Q. Broughton and P. S. Bagus, *Phys. Rev. B* **30**, 4761 (1984).